Materials Science and Engineering, R22 (1998) 57–78

Reports: A Review Journal

Self-monitoring structural materials

D.D.L. Chung *

Composite Materials Research Laboratory, State University of New York at Buffalo, Buffalo, NY 14260-4400, USA

Received 28 February 1997; accepted 22 September 1997

Abstract

Self-monitoring (or intrinsically smart) structural materials, including concrete containing short carbon fibers, and polymer-matrix and carbon-matrix composites containing continuous carbon fibers, were reviewed. Each material is capable of monitoring its own reversible strain and damage through the effects of these on the electrical resistance of the material. This capability is valuable for structural control and structural health monitoring. Among these three materials, the concrete gives the highest strain sensitivity or gage factor (up to 700), while the carbon–carbon composite gives the highest damage sensitivity (i.e., sensitivity even to the damage after the first cycle of tensile loading within the elastic regime). The origin of the self-monitoring ability differs among the three materials. For the concrete, it is related to slight fiber pull-out during strain and fiber and matrix fracture during damage. For the polymer-matrix composite, it is related to the increase in the degree of fiber alignment and reduction of fiber pre-stress during tension in the fiber direction and to fiber fracture and delamination during fatigue. For the carbon–carbon composite, it is related to dimensional changes during strain and fiber and matrix fracture during damage.

Keywords: Structural materials; Smart materials; Sensors; Self-monitoring; Strain; Damage; Composites

1. Introduction

Structural materials have evolved from materials that are mechanically strong (such as steel and concrete) to materials that are both strong and lightweight (such as composite materials) and most recently to materials that are both strong and self-monitoring. A self-monitoring material is one which can sense its own strain (including reversible strain) and damage. It can be considered a smart material. However, in contrast to smart materials such as optical fibers, piezoelectric sensors, etc., the self-monitoring materials are themselves structural materials. Thus, in contrast to structures rendered smart by embedded or attached sensors, self-monitoring structural materials are intrinsically smart, so that there is no need of embedded or attached sensors. Advantages of intrinsically smart structural materials compared to the use of embedded or attached sensors (extrinsic smartness) are (i) low cost, (ii) great durability, (iii) large sensing volume and (iv) absence of mechanical property degradation due to the embedding of sensors. The sensing of strain is valuable for structural control (for vibration damping) and dynamic load monitoring (for traffic control and automatic highways in case of concrete); the sensing of damage is valuable for structural health monitoring and service life prediction. Relevant industries include construction (in relation to self-monitoring concrete), aerospace (in relation to self-monitoring carbon fiber polymer-matrix composite and carbon–carbon composite) and automobile and sporting goods (in relation to self-monitoring carbon fiber polymer-matrix composite) industries.

Self-monitoring structural materials reviewed here include concrete with short carbon fibers [1–9], continuous carbon fiber polymer-matrix composite [10–12] and carbon–carbon composite with continuous carbon fibers [13]. Composites with short fibers and matrices other than cement are not

* Corresponding author.

0927-796X/98/$19.00
PII S0927-796X(97)00021-1

able to compete with their continuous fiber counterparts as structural materials, even though they are able to self-monitor and have their distinct origins of the self-monitoring ability, so these composites are not covered in this review [14–16]. Cost considerations make the use of continuous fibers in a cement matrix not practical. Akin to the continuous carbon fiber polymer-matrix composite is a polymer-matrix composite containing a combination of continuous glass fibers and continuous carbon fibers [17]. Not included in this review are a CaF_2-matrix SiC-whisker composite [18] and a Si_3N_4-matrix SiC-whisker composite [19], due to their less attractive sensing abilities and less common usage. All these composites contain one or more components that are electrically conducting. The polymer-matrix composite has conducting carbon fibers but a non-conducting polymer matrix; the concrete has conducting carbon fibers and a less conducting cement matrix; the carbon–carbon composite has conducting fibers and conducting matrix. That one (or more) component(s) in the composite is (are) conducting is a basic requirement for the self-monitoring ability, which is based on the dependence of the electrical resistance of the composite on the strain and damage of the composite. On the other hand, the matrix should not be highly conducting, as the low resistivity of the resulting composite will make the resistance changes too small to be conveniently detected. For this reason, metal-matrix composites do not have good self-monitoring ability.

The origin of the ability to sense reversible strain differs among the three types of composites mentioned above, though all origins relate to phenomena that are reversible. For the concrete with short carbon fibers, the origin is the slight (<1 μm) pull-out of electrically conducting short carbon fibers during slight crack opening and the consequent increase in the fiber-matrix electrical contact resistivity and increase in the volume resistivity of the composite. For the continuous carbon fiber polymer-matrix composite, the origin is the increase of the degree of alignment of fibers that are parallel to the stress axis and the reduction of the fiber pre-stress incurred during curing and cooling of the polymer matrix, and the consequent decrease of the volume electrical resistivity of the composite in the fiber direction and increase of the resistivity perpendicular to the fiber layers. For the carbon–carbon composite, the origin is the dimensional changes due to elastic deformation and the consequent increase in the volume electrical resistance (not resistivity) of the composite.

The origin of the ability to sense damage also differs among the three types of composites, though all origins relate to phenomena that are irreversible. For the concrete with short carbon fibers, the origin in the small damage regime is matrix damage, the consequent increase in the chance that adjacent fibers touch one another and the consequent decrease in the volume resistivity of the composite; and the origins in the large damage regime are fiber breakage and matrix cracking, and the consequent increase in the volume resistivity of the composite. For the continuous carbon fiber polymer-matrix composite, the origin is fiber breakage and the consequent increase in the volume resistivity of the composite in the fiber direction. For the carbon–carbon composite, the origin is matrix and fiber cracking and the consequent increase in the volume resistivity of the composite.

The abilities to sense reversible strain and damage are described below for each of the three types of self-monitoring structural materials mentioned above. The combined ability to monitor both reversible strain and damage is particularly valuable in real-time fatigue damage monitoring under dynamic loading which may or may not be periodic in time, because the strain cycle and the point within the cycle at which damage occurs can be identified.

This review covers the science of self-monitoring structural materials. This science is interdisciplinary, involving materials science and engineering, electrical engineering, mechanical engineering and civil engineering. Application of this science to structures having various shapes, dimensions and embedded components awaits the attention of both materials engineers and structural engineers. This application also involves data acquisition from the self-monitoring structures (spatially continuous, in contrast to the discreteness of embedded sensors), as well as subsequent data analysis and storage—

tasks requiring materials engineers and electrical engineers. This review does not cover the applications, but is intended to stimulate interdisciplinary work on both the science and applications of self-monitoring structural materials.

2. Self-monitoring concrete

Carbon fiber reinforced concrete is attractive for civil structures due to its high tensile and flexural strengths, high tensile ductility, high flexural toughness, low drying shrinkage [20–30], strain sensing ability [1–9] and low cost. This section focuses on its strain sensing ability. Damage sensing ability exists in this material, but it is not as powerful as the strain sensing ability.

Self-monitoring in concrete was achieved with concrete containing short, electrically conducting microfibers, preferably carbon fibers, in an amount as low as 0.2 vol %. The DC volume electrical resistivity of the concrete changes reversibly upon reversible strain, such that the fractional change in electrical resistance per unit strain (i.e., the strain sensitivity or the gage factor) reaches 700 (extraordinarily high compared to values around 2 for conventional resistive strain gages). The effect has been observed in cement paste, mortar as well as concrete, under tension, compression and flexure, though the effect is more pronounced in cement paste and mortar than in concrete. The reversible electromechanical effect stems from the reversible increase in the contact electrical resistivity between fiber and matrix upon slight opening (< 1 μm) of the crack which the fiber bridges (i.e., slight fiber pull-out), and the consequent reversible increase in the volume electrical resistivity of the cement-matrix composite [1–8].

The evidence in support of the above-mentioned origin of the self-monitoring ability of intrinsically smart concrete is summarized below.

(1) The sensing ability was present when the fibers were conducting (i.e., carbon or steel) and absent when the fibers were non-conducting (i.e., polyethylene) [5].

(2) The sensing ability was absent when fibers were absent [1,2,5,7].

(3) The sensing ability occurred even at low carbon fiber volume fractions, which were associated with little effect of the fiber addition on the concrete's volume electrical resistivity [5,31,32].

(4) There was no maximum volume electrical resistivity required in order for the sensing ability to be present [5].

(5) The sensing ability was present when the carbon fiber volume fraction was as low as 0.2% (below the percolation threshold) [5,7].

(6) Fracture surface examination showed that the fibers were separate from one another [5].

(7) The fractional increase in electrical resistance ($\Delta R/R_0$) upon straining essentially did not increase with increasing carbon fiber volume fraction, even though the increase in fiber volume fraction caused large decrease (by orders of magnitude) in the volume electrical resistivity [5].

(8) The electrical resistance increased upon tension (fiber pull-out) and decreased upon compression (fiber push-in), except for the first compressive strain cycle at 7 days of curing. The resistance change during the first strain cycle is consistent with the need to weaken the fiber-matrix interface prior to fiber pull-out in case the interface was relatively strong to start with [5,6,8].

(9) The presence of carbon fibers caused the crack height to decrease from ~ 100 μm (Fig. 1a) to < 1 μm (Fig. 1b), as observed after deformation to 70% of the compressive strength [7].

(10) The presence of carbon fibers caused the flexural toughness and tensile ductility of the composite to greatly increase [32,33].

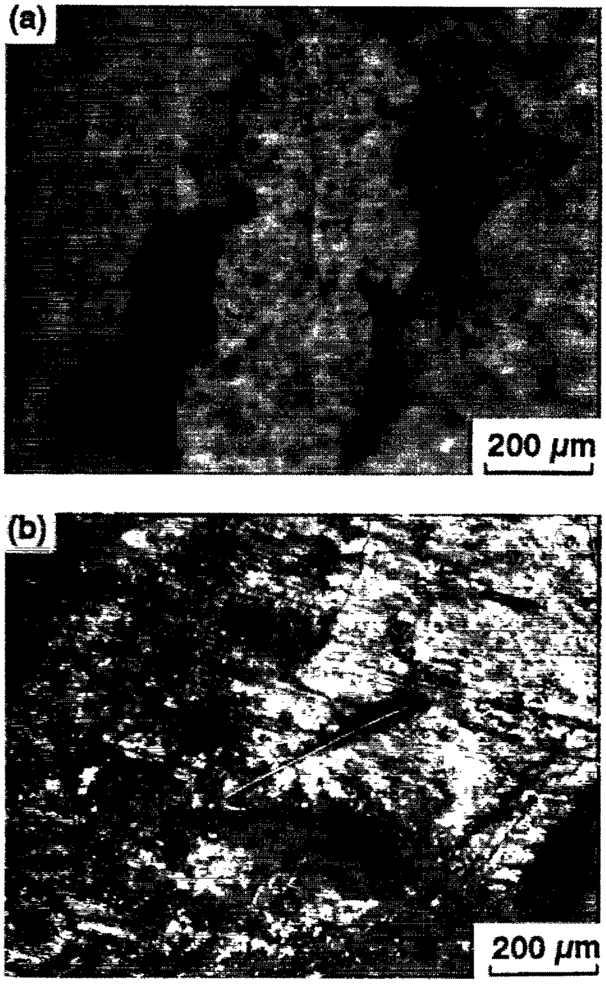

Fig. 1. Scanning electron microscope photographs of mortar after deformation to 70% of its compressive strength. (a) Mortar without fibers. (b) Mortar with carbon fibers. A crack in (b) is in the middle of the top quarter of (b), in the direction down the page, approximately. The two straight features in the center part of (b) are carbon fibers (10 μm diameter).

(11) The stress required for fiber pull-out in the short fiber composite was consistent with the shear bond strength between carbon fiber and cement paste, as obtained by single fiber pull-out testing [4].

(12) The contact electrical resistivity between carbon fiber and cement paste increased during debonding [4].

(13) The residual stress in a single carbon fiber embedded in cement paste is negligible.

Due to the small volume fraction of carbon fibers, the decrease of the concrete's volume electrical resistivity due to the fiber addition is small [5,31]. In order to help the fibers disperse, admixtures such as silica fume, methylcellulose and latex are used along with the fibers [31,32]. The fibers are the most inexpensive type of carbon fibers, namely those based on isotropic pitch. However, the fibers need to be surface treated with ozone in order to improve wetting with water, improve fiber dispersion in concrete, increase bond strength between fiber and cement matrix, and increase tensile strength, modulus and ductility of concrete relative to the values obtained with fibers that have not been treated [34–36]. The results given in this section were obtained using ozone treated carbon fibers, for cement-matrix composites cured for 28 days, unless stated otherwise.

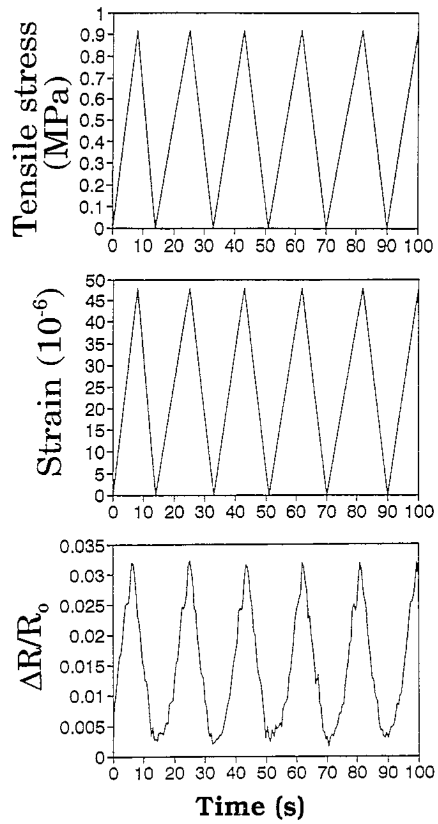

Fig. 2. $\Delta R/R_0$, strain and stress during first cyclic tensile loading of cement paste with ozone treated carbon fibers.

Due to the high electrical contact resistivity between steel rebar and concrete [37] and the low ability of an electrical current applied on one surface of a concrete structure to penetrate the concrete to depths more than 1 mm, the presence of steel rebars in concrete does not interfere with the performance of the self-sensing concrete around it unless the electrical contacts are around the whole cross-section of the concrete (rather than on one side) and unless the concrete is inside a cage made of the rebars.

Fig. 2 gives the fractional DC resistance increase ($\Delta R/R_0$) during first tensile loading of cement paste with 0.51 vol % carbon fibers at a stress amplitude of 0.9 MPa, or a strain amplitude of 4.8×10^{-5}, which was within the elastic regime. (The tensile strength was 2.23 MPa.) The resistance was in the stress direction. Both stress and strain returned to zero at the end of each cycle. The $\Delta R/R_0$ increased during tensile loading in each cycle and decreased during unloading in each cycle, with a gage factor (fractional change in resistance per unit strain) of 700. This is due to fiber pull-out during loading and fiber push-in during unloading. At the end of the first cycle, $\Delta R/R_0$ was positive rather than zero. This resistance increase is attributed to damage of the fiber–cement interface due to the fiber pull-out and push-in.

Fig. 3 gives $\Delta R/R_0$ during first cyclic compressive loading of mortar (with sand) with 0.24 vol % carbon fibers at a stress amplitude of 16 MPa, or a strain amplitude of 8×10^{-4}, which was within the elastic regime. The resistance was in the stress direction. Both stress and strain returned to zero at the end of each cycle. The $\Delta R/R_0$ decreased during compressive loading in each cycle and increased during unloading in each cycle, with a gage factor of 560. This is due to fiber push-in during loading and fiber pull-out during unloading. At the end of the first cycle, $\Delta R/R_0$ was positive rather than zero.

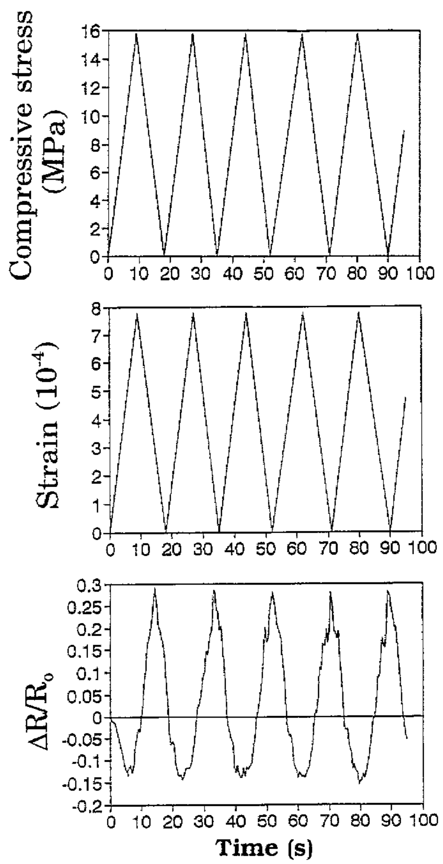

Fig. 3. $\Delta R/R_0$, strain and stress during first cyclic compressive loading of mortar with ozone treated carbon fibers.

This resistance increase is attributed to damage of the fiber–cement interface due to the fiber push-in and pull-out.

If as-received rather than ozone treated carbon fibers were used, the results are similar except that, as cycling progresses, both the maximum $\Delta R/R_0$ and minimum $\Delta R/R_0$ in a cycle decreases, as shown in Figs. 4 and 5 for tension and compression respectively. This is attributed to damage of the cement matrix separating adjacent fibers at their junction; this damage increases the chance for adjacent fibers to touch one another, thereby decreasing the resistivity. This decrease from cycle to cycle persists for the first 120–350 cycles (about 10% of fatigue life), after which the maximum and minimum $\Delta R/R_0$ do not change with cycling. Since the ozone treatment of the carbon fibers improves the mechanical properties of the composite [35] and the decrease in resistance from cycle to cycle (Figs. 4 and 5) is due to damage of the cement matrix, it is reasonable that the ozone treatment removes the decrease in resistance from cycle to cycle. Another difference is that the gage factor is higher when ozone treated fibers are used. In Fig. 4, the gage factor is 625 (less than the value of 700 in Fig. 2). In Fig. 5, the gage factor is 500 (less than the value of 560 in Fig. 3).

Upon static compression up to failure, the resistance decreased monotonically; upon static tension up to failure, the resistance increased monotonically. These trends are consistent with those in Figs. 2–5 for cyclic loading.

During the few cycles before fatigue failure at 28 days of curing, the resistance did not increase irreversibly and significantly, indicating that the mortar is poor in its ability to monitor damage. This

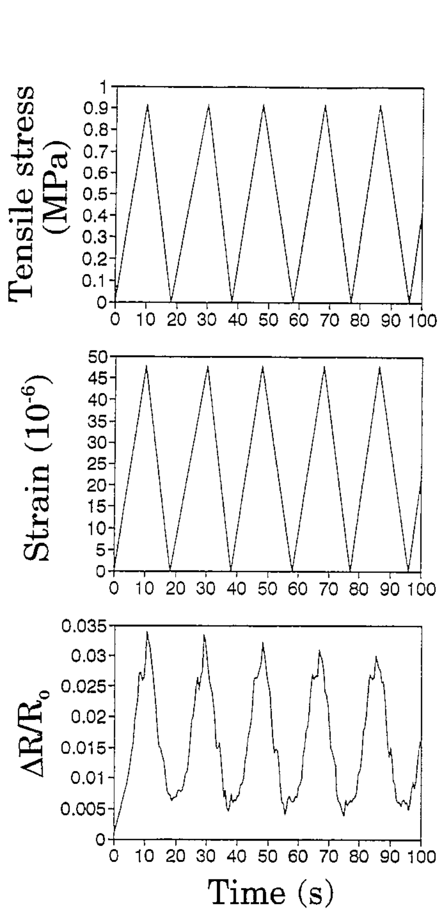

Fig. 4. $\Delta R/R_0$, strain and stress during first cyclic tensile loading of cement paste with as-received carbon fibers.

poor damage sensitivity is also reflected by the absence of a resistance increase prior to static compressive failure.

Results under tension and compression were similar, except that tensile loading caused resistance increase due to fiber pull-out and compressive loading caused resistance decrease due to fiber push-in. Due to the much lower ductility under tension than under compression, the fractional change in resistance at fracture is much lower under tension than under compression [7]. Figs. 2–5 were obtained with the resistance in the stress direction. The tensor relationship between the resistance and strain in different directions still need to be determined. Figs. 2–5 give the overall resistance of the sample, but the placement of more than two voltage probes allows measurement of the resistivity distribution. Resistivity tomography may be used to obtain a two-dimensional resistivity distribution.

Figs. 2–5 were obtained under DC condition. Similar results were obtained under AC condition [9]. The fractional increase in reactance can be larger than the fractional increase in resistance under the same load. However, the difference is not very large and AC measurement requires more expensive equipment than DC measurement. Therefore, DC operation is recommended, unless data acquisition using wireless methods is desired.

3. Self-monitoring carbon fiber polymer-matrix composite

Continuous carbon fiber polymer-matrix composite is an advanced composite which is attractive in its combination of high strength, high modulus and low density. It is widely used for aerospace

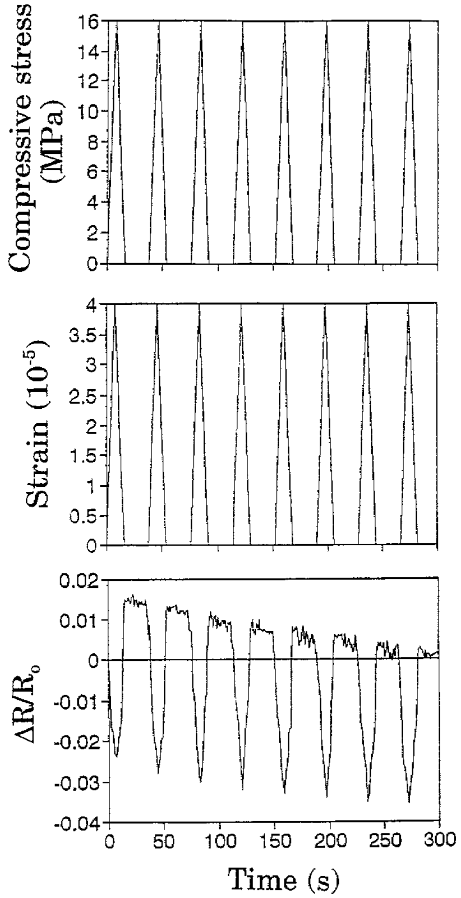

Fig. 5. $\Delta R/R_0$, strain and stress during first cyclic compressive loading of mortar with as-received carbon fibers.

structures, sporting goods and other lightweight structures. For a polymer-matrix composite containing a combination of continuous glass fibers and continuous carbon fibers, the electrical resistance increases irreversibly upon damage (due to the fracture of the carbon fibers) [17], but fatigue monitoring and reversible resistivity changes (dynamic strain monitoring) were not explored. For a continuous carbon fiber polymer-matrix composite [10,11], it has been shown that both the longitudinal (fiber or stress direction) and transverse (through-thickness) electrical resistivities of the composite change reversibly upon dynamic straining and change irreversibly upon fatigue damage. In other words, a continuous carbon fiber polymer-matrix composite is self-monitoring.

Fig. 6 shows the fractional DC resistance increase ($\Delta R/R_0$), tensile stress and tensile strain simultaneously obtained in the stress (fiber) direction during cyclic tension–tension loading of a unidirectional carbon fiber epoxy-matrix composite with 8 fiber layers [11]. The resistance was measured by using the four-probe method, with silver paint for the electrical contacts. The strain did not return to zero at the end of each cycle. The resistance R decreased upon loading and increased upon unloading in every cycle, such that R irreversibly decreased after the first cycle, as for the case of the strain being completely reversible. The irreversible decrease in R after the first cycle (even when the strain is completely reversible) is due to the irreversible decrease in the degree of neatness of the fiber arrangement. A length increase without any resistivity change would have caused R to increase during tensile loading. In contrast, R was observed to decrease (not increase) upon tensile loading. Furthermore, the observed magnitude of $\Delta R/R_0$ was 9–14 times that of $\Delta R/R_0$ calculated by assuming

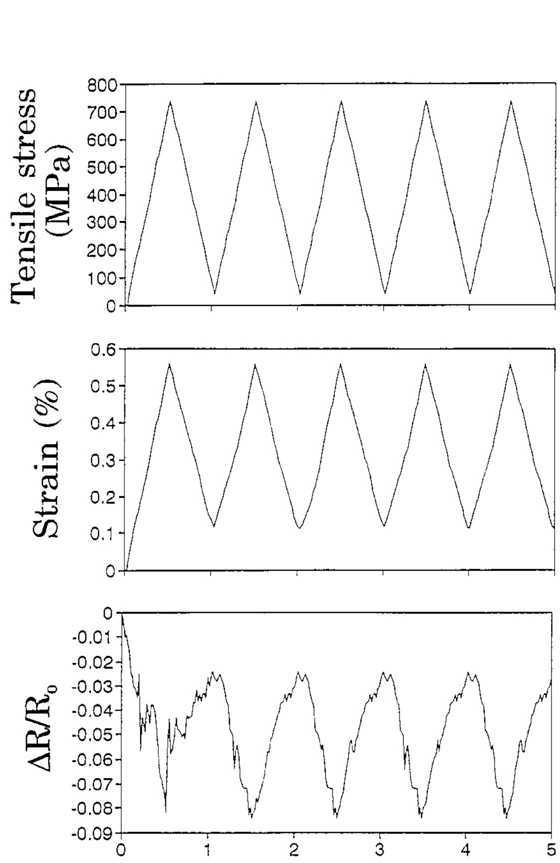

Fig. 6. Variation of fractional resistance increase ($\Delta R/R_0$), tensile stress and tensile strain with cycle number during the first few cycles of tension–tension fatigue testing for a unidirectional [0] carbon fiber polymer-matrix composite.

that $\Delta R/R_0$ was only due to length increase and not due to any resistivity change. Hence, the contribution of $\Delta R/R_0$ from the length increase is negligible compared to that from the resistivity change. The reversible decrease in R was attributed partly to increase in the degree of fiber alignment (e.g., slightly off-axis fibers becoming more aligned with the stress) and partly to the reduction of the compressive pre-stress in the fiber [31]. The pre-stress and the resulting fiber resistance increase (by 10%) occur after the curing and cooling of the epoxy around the fiber, since the epoxy shrinks upon curing and cooling. Subsequent tension causes reduction of the pre-stress and hence decrease (by 10%) of the fiber resistance [38].

As cycling progressed beyond 218,277 cycles (or 55% of fatigue life), the peak R (at the end of a cycle) significantly but gradually increased, such that the increase did not occur in every cycle, but occurred in spurts (Figs. 7 and 8a), e.g., at 218,278 cycles (Fig. 7c) and 229,628 cycles (Fig. 7d). Fig. 8 shows the variation of the peak $\Delta R/R_0$ as a function of the percentage of the fatigue life throughout the entire life. Beyond 353,200 cycles (89% of fatigue life), the increase of the peak R occurred continuously from cycle to cycle rather than in spurts (Fig. 7e). At 396,457 cycles (99.9% of fatigue life), the increase became more severe, such that spurts of increase occurred on top of the continuous increase (Fig. 8b). The severity kept increasing until failure at 396,854 cycles, at which R abruptly increased. The last spurt before the final abrupt increase occurred at 396,842 cycles (99.997% of the fatigue life) (Fig. 7e).

The early period in which the peak R increased discontinuously in spurts is attributed to minor damage in the form of fiber breakage which did not occur in every cycle. The subsequent period in

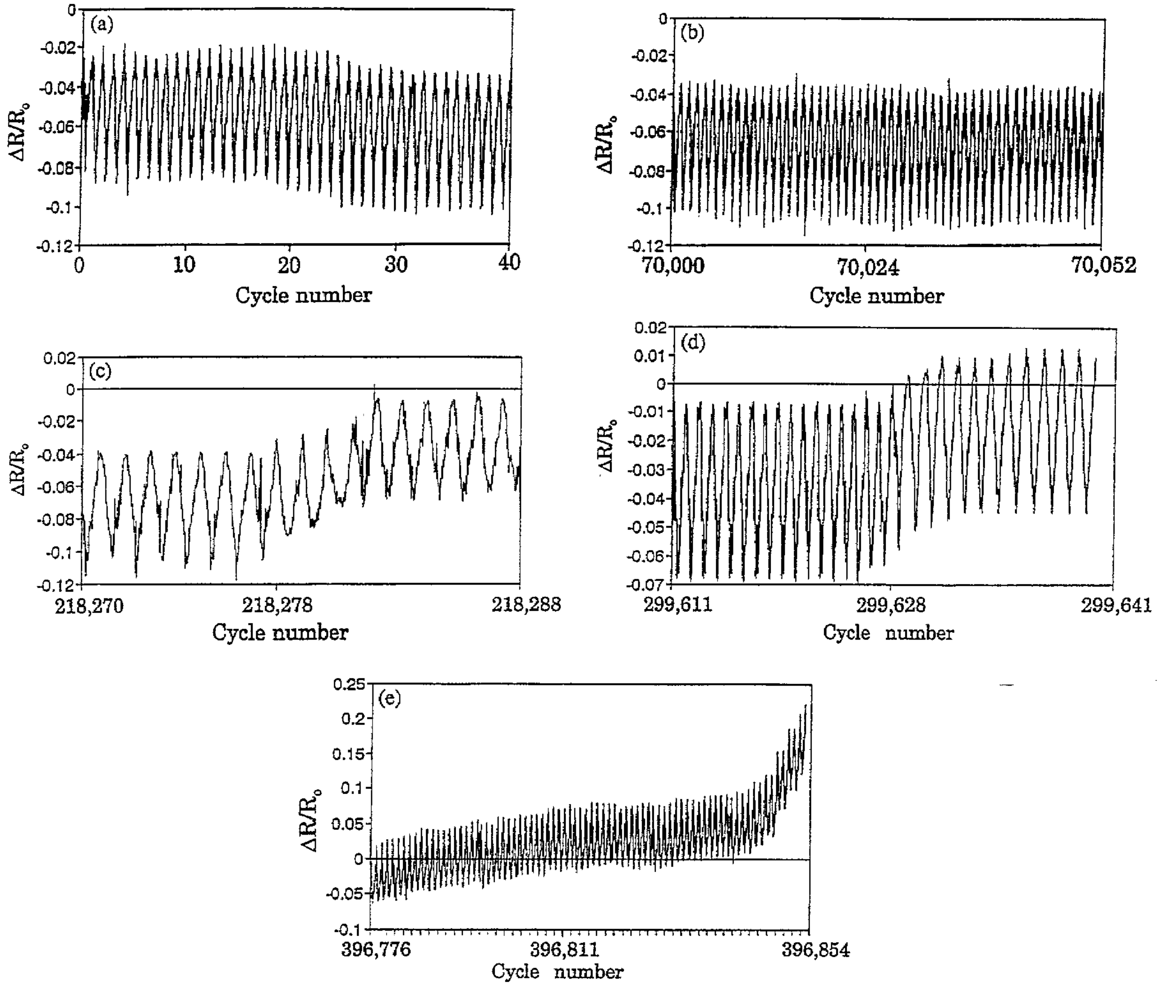

Fig. 7. Variation of $\Delta R/R_0$ with cycle number during tension–tension fatigue testing up to failure at 396,854 cycles for a unidirectional [0] carbon fiber polymer-matrix composite.

which the peak R increased continuously but gradually is attributed to fiber breakage which occurred in every cycle. The still subsequent period in which the peak R increased rapidly, both in spurts (which did not occur in every cycle) and continuously (i.e., in every cycle), is attributed to more extensive fiber breakage, which occurred in the final period before failure. Thus, by following the increase in the peak R, the degree of damage can be monitored progressively in real time. Moreover, progressive warning of the impending fatigue failure is provided in real time, so disasters due to fatigue failure can be avoided.

Single fibers obtained by dissolving away the polymer from the carbon fiber prepreg were subjected to similar electromechanical testing [39]. The resistance R of a single fiber increased upon tension, such that at a tensile stress equal to 83.0% of the fracture stress, the reversible portion of $\Delta R/R_0$ (due to dimensional change) was 18.4×10^{-3}, while the irreversible portion of $\Delta R/R_0$ (due to damage) was 4.0×10^{-3} [39]. It was therefore assumed that a fiber prior to fatigue failure has an irreversible $\Delta R/R_0$ of 4.0×10^{-3}. There are two sources of irreversible $\Delta R/R_0$, namely fiber damage and fiber breakage, though the former was almost negligible compared to the latter. The irreversible $\Delta R/R_0$ due to fiber damage was subtracted from the measured irreversible $\Delta R/R_0$ (in the part of the

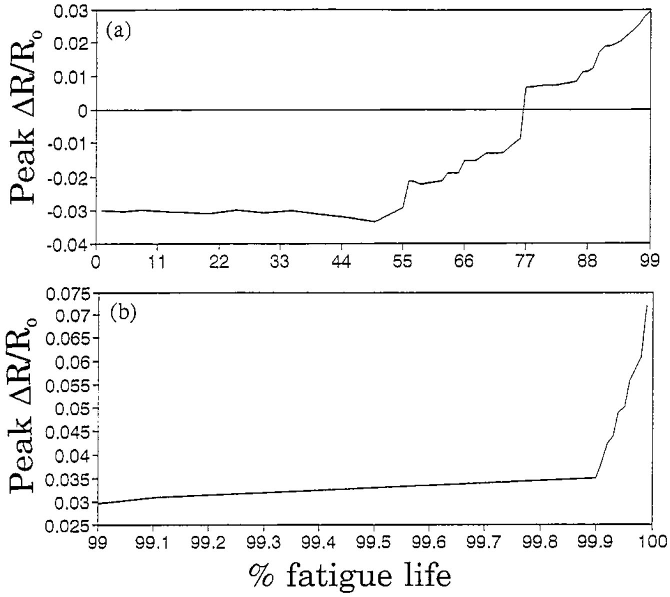

Fig. 8. Variation of the peak $\Delta R/R_0$ at the end of a cycle with the percentage of fatigue life during tension–tension fatigue testing up to failure for a unidirectional [0] carbon fiber polymer-matrix composite.

fatigue life in which the irreversible $\Delta R/R_0$ had shown an increase from the initial value) in order to obtain the irreversible $\Delta R/R_0$ due to fiber breakage.

Assuming that the resistivity of the undamaged portion of the composite does not change during testing, the fraction of fibers broken is equal to the fractional decrease in the effective cross-sectional area of the unidirectional composite. Hence, in the part of the fatigue life in which the peak R at the end of a cycle had shown an increase from its value R_0' at the end of the first cycle ($R_0' = R_0 + (\Delta R)_0$, where R_0 is the initial resistance and $(\Delta R)_0$ is the ΔR at the end of the first cycle),

$$\text{fraction of fibers broken} = \frac{Q}{1+Q}, \tag{1}$$

where $Q = ((R - R_0')/(R_0')) - 4.0\times10^{-3}$, R is the peak R at the end of a cycle, and 4.0×10^{-3} is the contribution from fiber damage. Fig. 9 shows a plot of the fraction of fibers broken as a function of the percentage of fatigue life, as obtained by using Eq. (1). Although not shown in Fig. 9, the breaking of fibers was accompanied by a decrease in the secant tensile modulus, which was continuously monitored during fatigue testing. Fiber breakage started to occur at 50% of the fatigue life, though appreciable growth of the fraction of fibers broken did not start till 55% of the fatigue life. Fiber breakage occurred in spurts from 55% to 89% of the fatigue life, due to fiber breakage not occurring in every cycle. The smallest spurt involved 0.006 of the fibers breaking. This corresponds to 1020 fibers breaking. Thus, each spurt involved the breaking of multiple fibers. This is reasonable since the fibers were in bundles of 6000 fibers. The smallest spurt involved the breaking of a fraction of a fiber bundle. At 89% of the fatigue life, fiber breakage started to occur continuously rather than in spurts. Catastrophic failure occurred when 18% of the fibers were broken.

Figs. 6–9 pertain to the resistance in the stress (fiber) direction. Although the polymer matrix is electrically insulating, the resistance perpendicular to the fiber layers (i.e., in the direction through the thickness of the composite) is not ∞, due to contacts between fibers in adjacent layers. This resistance changes in the opposite direction from the resistance in the fiber direction, when tensile stress is applied in the fiber direction. In other words, the resistance perpendicular to the fiber layers increases reversibly

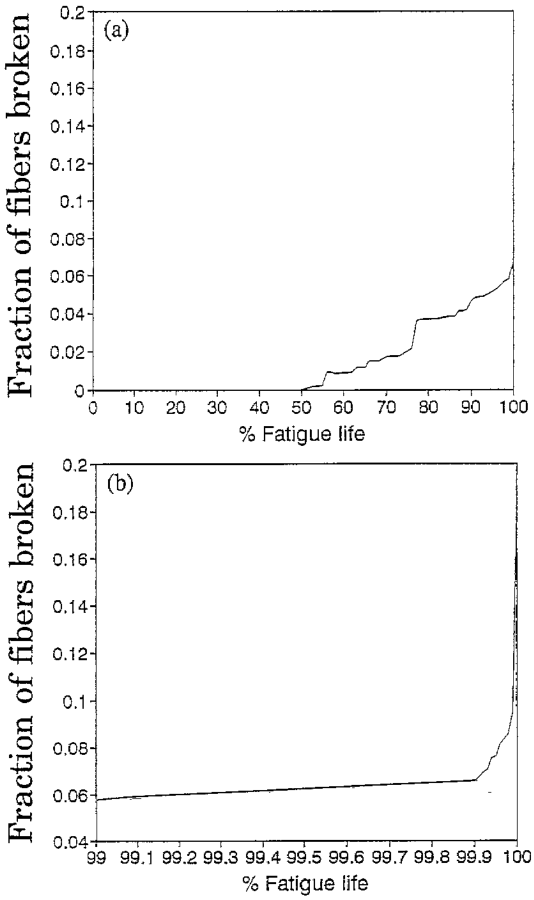

Fig. 9. Variation of the fraction of fibers broken with the percentage of fatigue life during tension–tension fatigue testing up to failure for a unidirectional [0] carbon fiber polymer-matrix composite. (a) From 0% to 100% of fatigue life. (b) From 99% to 100% of fatigue life.

upon tension in the fiber direction. This is because of the inherent waviness (marcelling) of the fibers in each layer and the decrease in the degree of waviness and the consequent decrease in the chance that adjacent fiber layers touch one another, as stress is applied in the fiber direction. This reversible electromechanical effect provides a way to assess the degree of fiber waviness. Upon fatigue loading in the fiber direction, delamination causes the through-thickness resistance to increase irreversibly. Fig. 10 gives the fraction of cross-sectional area delaminated during fatigue testing for a crossply [0/90] composite, as calculated from the irreversible resistance increase. Delamination started at 33% of the fatigue life and abruptly grew at 62% of the fatigue life, so that 4.3% of the area was delaminated.

Figs. 6–9 are for a unidirectional [0] composite. Similar results were obtained for a crossply [0/90] composite, except that the effect is less due to the presence of the 90° fiber layers. For a unidirectional [90] composite (i.e., stress perpendicular to the fibers in the plane of the fiber layers), the results are different, as the resistance increases upon tension and decreases upon compression (Figs. 11 and 12) due to the change in proximity between the adjacent fibers; the effect is almost totally reversible and is much more linear than for the [0] and [0/90] composites, but the strain sensitivity is lower than those of the [0] and [0/90] composites.

Figs. 6–9 describe the behavior during tension for the unidirectional [0] composite. Similar behavior but in the opposite direction occurs during compression. For example, the resistance in the

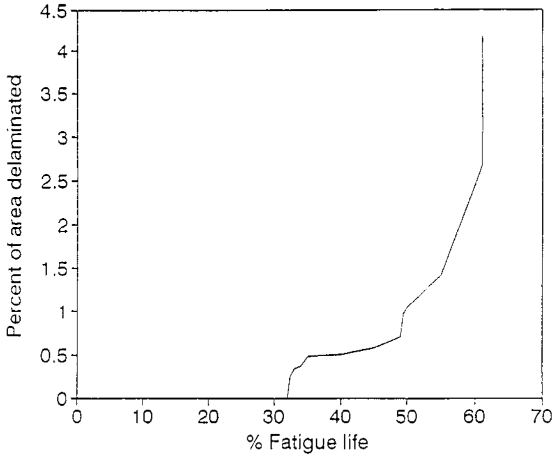

Fig. 10. Fraction of cross-sectional area delaminated during fatigue testing of a crossply [0/90] carbon fiber polymer-matrix composite.

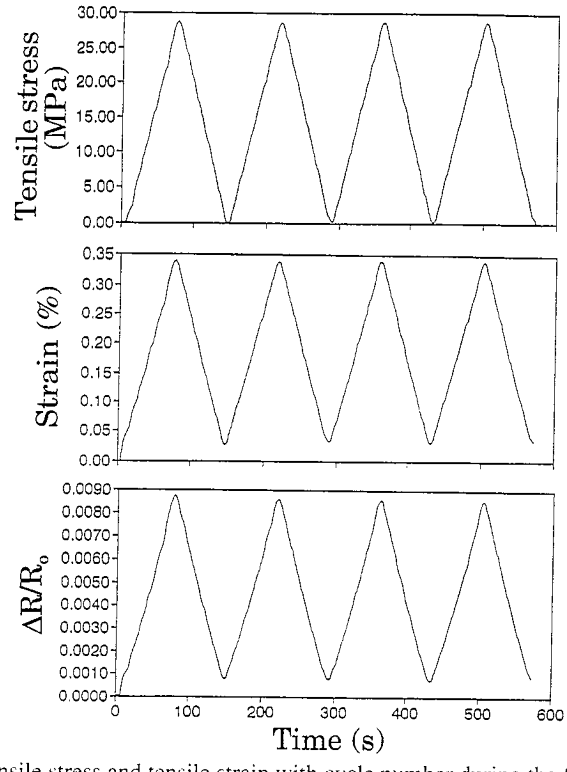

Fig. 11. Variation of $\Delta R/R_0$, tensile stress and tensile strain with cycle number during the first few cycles of tensile loading for a unidirectional [90] composite.

stress (fiber) direction decreases upon tension and increases upon compression. Hence, the composite is self-monitoring under both tension and compression.

The strain sensitivity is up to 38 in magnitude in the fiber direction and up to 49 in the through-thickness direction for the unidirectional composite. The less aligned are the fibers in the composite prior to tension (i.e., the higher the electrical resistivity and the lower the tensile modulus of the composite in the fiber direction), the greater the tensile strain sensitivity in both fiber direction and

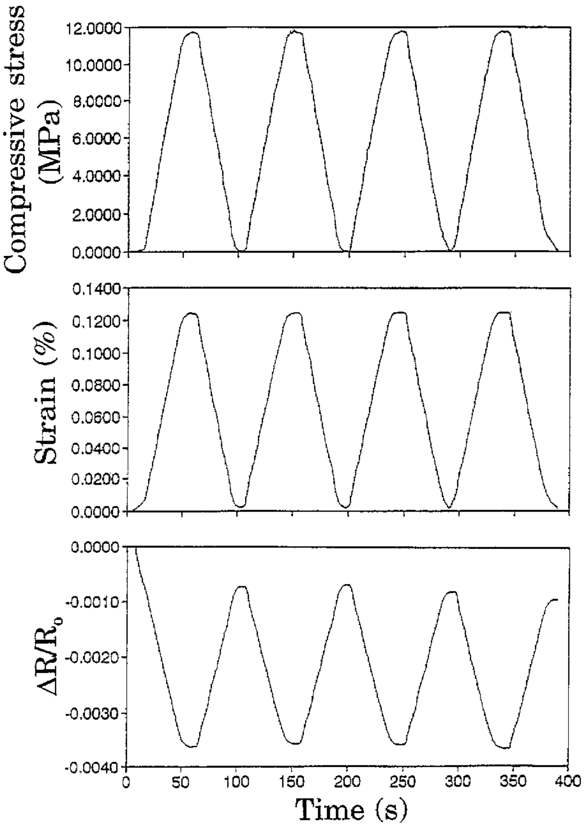

Fig. 12. Variation of $\Delta R/R_0$, compressive stress and compressive strain with cycle number during the first few cycles of compressive loading for a unidirectional [90] composite.

through-thickness direction [10]. The sensing of strain in the fiber (stress) direction can be performed by measuring either the resistance in the fiber (stress) direction or that in the through-thickness direction, depending on which direction makes the placement of the electrical contacts (four-probe method) on the composite structure more convenient. However, the sensing of damage in the form of fiber damage should be performed by measuring the resistance in the fiber (stress) direction and the sensing of damage in the form of delamination should be performed by measuring the resistance in the through-thickness direction. Although the strain sensitivity is not as good as that of self-monitoring mortar, it is much better than those of conventional resistive strain gages. On the other hand, the damage sensitivity is much better than that of self-monitoring mortar.

Figs. 6–11 were obtained by measuring the DC electrical resistance. No additional information was obtained by measuring the AC impedance, as the reactance is negligible compared to the resistance in these continuous fiber composites.

Polymer-matrix composites with short carbon fibers are also self-monitoring [14–16], but the origins of their self-monitoring ability differ from those of the continuous fiber composites mentioned above. The most common origin of the self-monitoring ability of short carbon fiber polymer-matrix composites is that tension causes the separation between adjacent fibers to increase, so that the resistivity increases, and compression causes this separation to decrease, so that the resistivity decreases.

4. Self-monitoring carbon–carbon composite

Carbon–carbon composites with continuous carbon fibers and a carbon matrix are used for high-temperature aerospace structures and biomedical implants, due to the high-temperature resistance and biocompatibility of carbon. The carbon matrix, though much more high-temperature resistant than a polymer matrix, is much more brittle than a polymer matrix. This brittleness makes carbon–carbon composites prone to matrix cracking. As a result, there is a need for monitoring the condition or health of a carbon–carbon composite structure while the structure is in use, in order to minimise hazards. This monitoring is conventionally conducted by acoustic emission, which is capable of detecting substantial cracking, but not slight cracking. Exceptional sensitivity to even slight damage can be obtained by using the carbon–carbon composite itself as the damage sensor to monitor the composite's own damage (i.e., to self-monitor the damage), using the increase in electrical resistivity as a measure of the irreversible composite damage [13]. The high sensitivity to damage is due to the high conductivity of the carbon matrix, compared to the cement and polymer matrices, and the importance of matrix cracking in the mechanism for damage in a carbon–carbon composite.

A structure experiences reversible strain during use. The monitoring of the strain is useful for control of the structure, so as to make the structure 'smart'. Embedded or attached strain sensors are conventionally used for the strain monitoring. These sensors can be optical fibers and a variety of strain gages. For a high-temperature structure, such as one made of a carbon–carbon composite, the sensors must be able to withstand high temperatures. Even if the temperature resistance is not a problem, the sensors suffer from poor durability and, in the case of embedded sensors, they have the tendency to degrade the mechanical properties of the structure. The carbon–carbon composite itself is a strain sensor, based on the reversible increase of the electrical resistance (not resistivity) of the composite upon tensile straining [13].

Fig. 13 shows the stress (curve (a)) and the fractional DC resistance increase ($\Delta R/R_0$) (curve (b)) obtained during static tension up to failure for a carbon–carbon composite having two-dimensionally (90°) woven fibers and a heat treatment temperature of 2000°C, with the resistance and stress in the direction of one of the two perpendicular sets of fibers. $\Delta R/R_0$ increased monotonically with

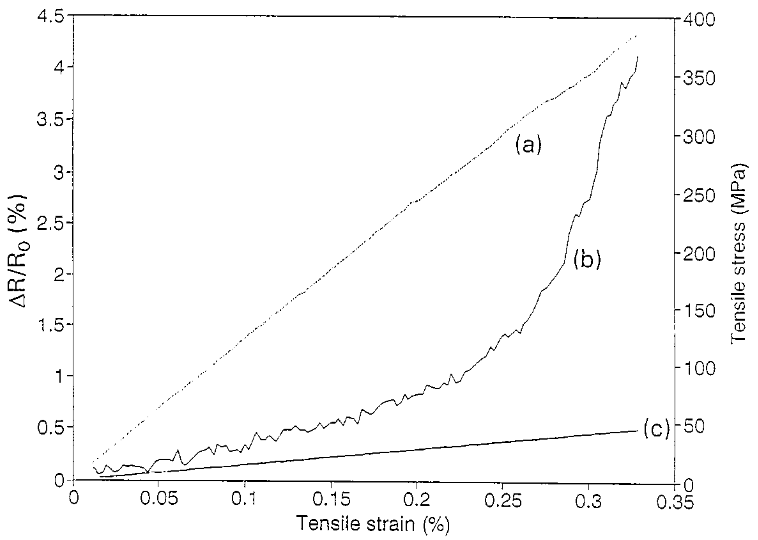

Fig. 13. Plots of (a) tensile stress vs. strain, and (b) $\Delta R/R_0$ vs. strain, obtained simultaneously during static tension up to failure for a carbon–carbon composite. Curve (c) is the calculated $\Delta R/R_0$ based on dimensional changes.

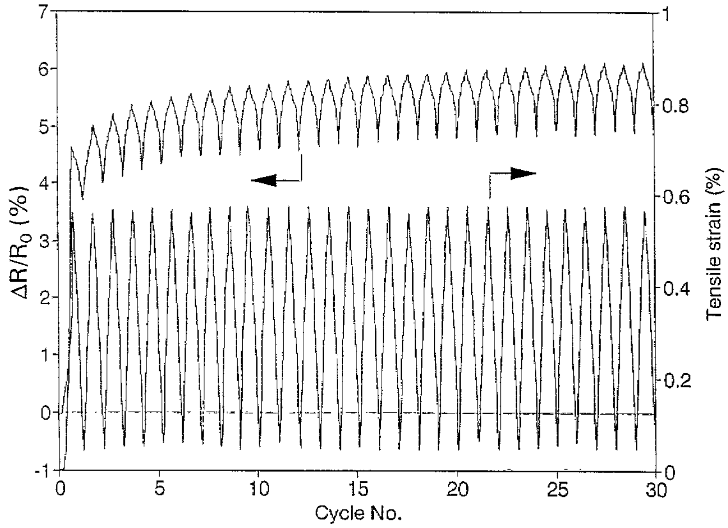

Fig. 14. Plots of $\Delta R/R_0$ vs. cycle No. and of tensile strain vs. cycle No., obtained simultaneously during first cyclic tension at a stress amplitude of 94% of the fracture stress for a carbon–carbon composite.

strain, such that the increase was gradual (only slightly above the increase in $\Delta R/R_0$ due to the changes in dimensions, curve (c) in Fig. 13) at low strains and abrupt at high strains.

Fig. 14 shows $\Delta R/R_0$ obtained during cyclic tension to a stress amplitude (360 MPa) equal to 94% of the breaking stress. The tensile strain was almost totally reversible. The irreversible strain was 0.040% at the end of the first cycle, and increased very slightly with increasing cycle number. $\Delta R/R_0$ increased upon loading in every cycle, such that it irreversibly increased slightly after every cycle and the irreversible increase in $\Delta R/R_0$ was particularly large for the first cycle, as shown in Fig. 14. At fatigue failure, $\Delta R/R_0$ abruptly increased, such that $\Delta R/R_0$ did not more rapidly increase irreversibly near the end of fatigue life. Fig. 15 shows the peak $\Delta R/R_0$ values in a cycle as a function of cycle number throughout the fatigue life up to failure. The peak $\Delta R/R_0$ increased with cycle number significantly during the first 500 cycles and gradually during all subsequent cycles up to failure. The

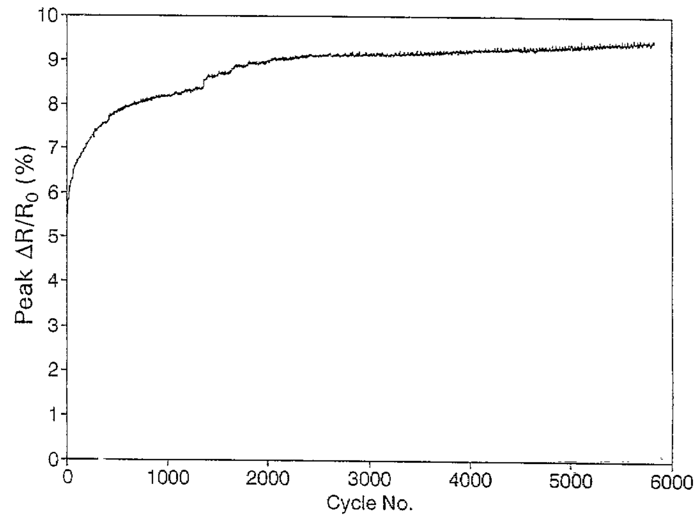

Fig. 15. Variation of the peak $\Delta R/R_0$ with cycle No. throughout the entire fatigue life at a stress amplitude of 94% of the fracture stress for a carbon–carbon composite.

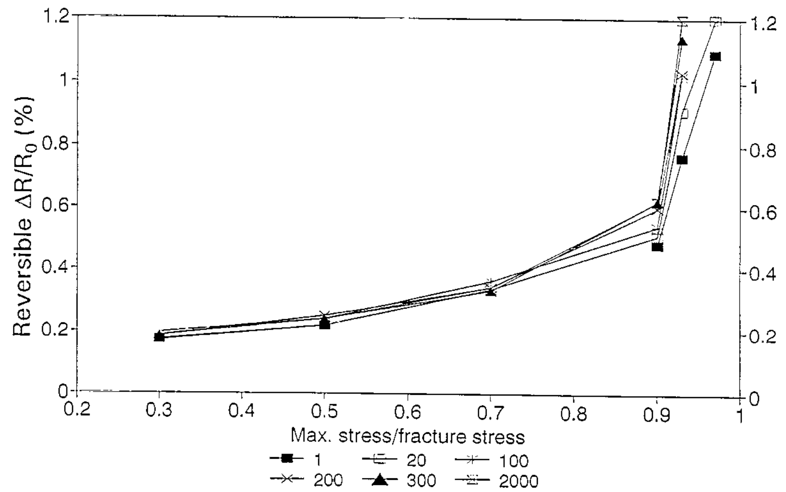

Fig. 16. Variation of the reversible part of $\Delta R/R_0$ with stress amplitude (fraction of fracture stress) for various fixed cycle numbers (i.e., 1, 20, 100, 200, 300 and 2000) for a carbon–carbon composite.

small step increases in the peak $\Delta R/R_0$, for example at ~1350 cycles, are not experimental artifacts but are attributed to damage occurring at those cycle numbers, similar to the step increases observed for a continuous carbon fiber polymer-matrix composite under similar cyclic loading [11].

The reversible part of $\Delta R/R_0$ increased significantly with increasing stress amplitude, and less significantly with increasing cycle number, as shown in Fig. 16. The irreversible part of $\Delta R/R_0$ was much smaller than the reversible part of $\Delta R/R_0$ at the lowest stress amplitude (30% of fracture stress), but exceeded the reversible part of $\Delta R/R_0$ at higher stress amplitudes. The irreversible part of $\Delta R/R_0$ increased with stress amplitude much more significantly than the reversible part of $\Delta R/R_0$ for the whole range of stress amplitudes studied. As the stress amplitude was increased beyond 90% of the fracture stress, both the reversible part (Fig. 16) and irreversible part (Fig. 17) of $\Delta R/R_0$ increased abruptly. Both the reversible and irreversible parts of $\Delta R/R_0$ increased with cycle number, but the effect was small compared to the effect of the stress amplitude (Figs. 16 and 17). The reversible strain increased with increasing stress amplitude linearly up to a stress amplitude of 90% of the fracture

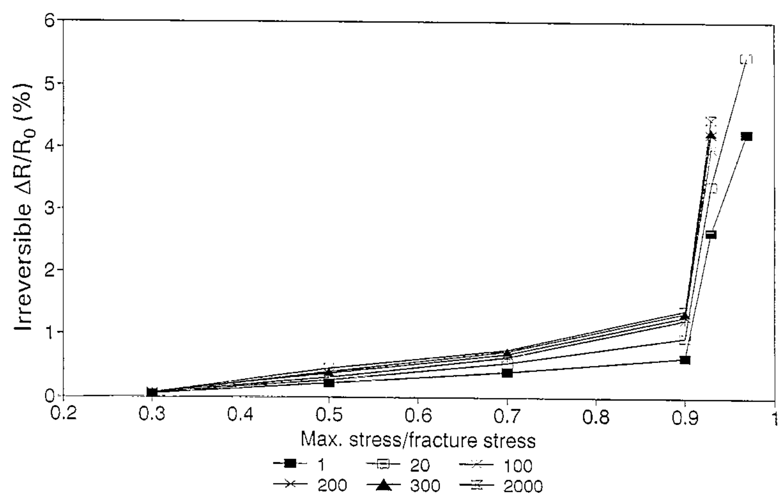

Fig. 17. Variation of the irreversible part of $\Delta R/R_0$ with stress amplitude (fraction of fracture stress) for various fixed cycle numbers (i.e., 1, 20, 100, 200, 300 and 2000) for a carbon–carbon composite.

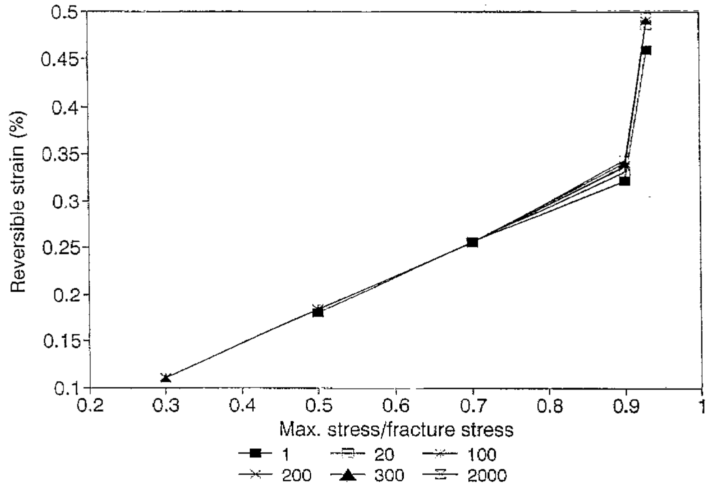

Fig. 18. Variation of the reversible strain with stress amplitude (fraction of fracture stress) for various fixed cycle numbers (i.e., 1, 20, 100, 200, 300 and 2000) for a carbon–carbon composite.

stress and abruptly increased upon further increase of the stress amplitude (Fig. 18). The magnitude of the irreversible strain was much lower than that of the reversible strain at all stress amplitudes. Both reversible and irreversible strains increased with cycle number, but the effect of both is small compared to the effect of the stress amplitude.

Fig. 19 shows the relationships between $\Delta R/R_0$ (reversible and irreversible) and reversible strain at a fixed cycle number (2000). The reversible part of $\Delta R/R_0$ (curve (b)) exceeded the calculated $\Delta R/R_0$ (based on the reversible dimensional changes, curve (c)) when the reversible strain exceeded 0.35%.

The reversible part of $\Delta R/R_0$ is mainly due to reversible dimensional changes and correlates with reversible strain. The irreversible part of $\Delta R/R_0$ is due to damage. Although the decreases in irreversible strain and Young's modulus also indicate damage, the changes in these parameters are very small

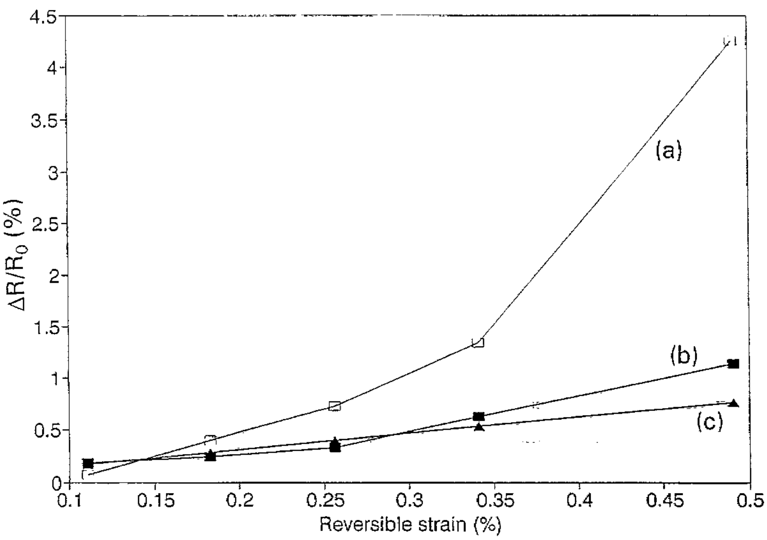

Fig. 19. Variation of $\Delta R/R_0$ with reversible strain for cycle 2000 for a carbon–carbon composite. (a) Irreversible part of $\Delta R/R_0$. (b) Reversible part of $\Delta R/R_0$. (c) Calculated $\Delta R/R_0$ based on reversible dimensional changes.

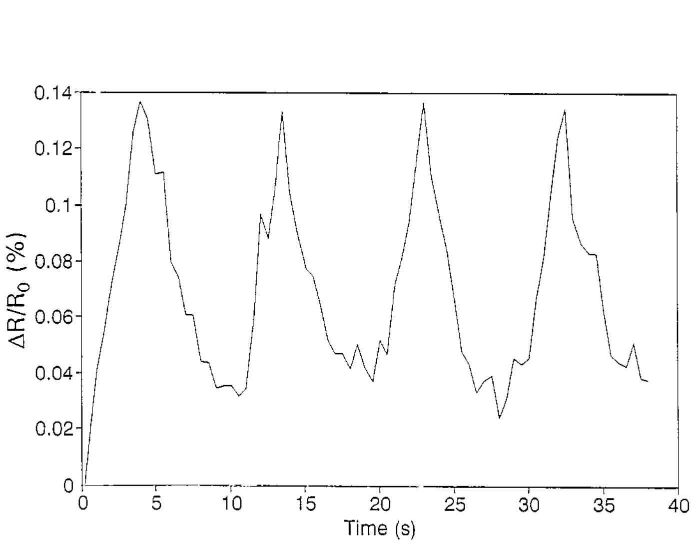

Fig. 20. Plot of $\Delta R/R_0$ vs. time during the first four cycles at a stress amplitude of 20% of the fracture stress for a carbon–carbon composite.

compared to the change in the irreversible part of $\Delta R/R_0$. The great sensitivity of the irreversible part of $\Delta R/R_0$ to damage is also shown by the significant non-zero value of the irreversible part of $\Delta R/R_0$ after merely the first cycle, even at a stress amplitude of just 20% of the fracture stress (Fig. 20). However, the incremental rise in irreversible $\Delta R/R_0$ beyond ~500 cycles was small. The composite damage probably involved fiber-matrix interface weakening, matrix cracking and fiber breakage; these origins of damage could not be distinguished through the experimental technique used. Nevertheless, the increase of the irreversible part of $\Delta R/R_0$ as cycling progressed provided a continuous indication of the extent of damage. That the reversible part of $\Delta R/R_0$ also increased with cycling and that an abrupt increase of the irreversible part of $\Delta R/R_0$ is associated with an abrupt increase in the reversible part of $\Delta R/R_0$ (Figs. 16 and 17) suggest that the reversible part of $\Delta R/R_0$ is partly associated with a phenomenon which intensifies as damage increases, although it is mostly associated with dimensional changes. This phenomenon may be reversible crack opening during tension, as cracks are expected to increase in size and/or density as cycling progresses. This interpretation is consistent with the observation that an abrupt increase in the reversible part of $\Delta R/R_0$ is associated with an abrupt increase in reversible strain (Figs. 16 and 18) and that the abrupt increase in reversible strain occurs at stress amplitudes beyond the range in which the reversible strain is linear in relation to the stress amplitude (Fig. 17). As a result of this phenomenon, the gage factor (reversible $\Delta R/R_0$ per unit reversible strain) increases slightly with cycle number. The dependence of the gage factor on the cycle number complicates the practical use of the carbon–carbon composite as a strain sensor.

5. Strain sensitivity and fatigue damage sensitivity of self-monitoring structural materials in comparison

The strain sensitivity is defined as the ratio of the reversible part of $\Delta R/R_0$ to the strain amplitude. It is the same as the gage factor. Its value under tension is shown in Table 1 for the various composites. It is exceptionally high for the cement-matrix composite and lowest for the carbon-matrix composite. Table 1 also shows the fatigue damage sensitivity in terms of the range of fatigue life that can be sensed. The larger is the range, the better is the fatigue damage sensitivity. The carbon-matrix composite is the best in fatigue damage sensitivity, while the cement-matrix composite is the worst. The differ-

Table 1
Tensile strain and fatigue damage sensitivity of various self-monitoring composites containing carbon fibers

Matrix	Strain sensitivity	Range of fatigue life sensed
Cement	700	0–10%
Polymer	−38 to −6 (in fiber direction)	50–100%
Carbon	1.2–2.4	0–100%

ences in strain/damage sensitivity are mainly due to the difference in origin of the sensing ability among the different composites.

The damage sensitivity of self-monitoring carbon–carbon composites is superior to that of self-monitoring continuous carbon fiber epoxy-matrix composites [10,11], which, by resistance measurement in the fiber direction, provide damage self-monitoring ability through the irreversible resistivity increase associated with fiber breakage, and, by resistance measurement in the through-thickness direction, provide damage self-monitoring ability through the irreversible resistivity increase associated with delamination. Due to the insulating character of the epoxy matrix, the epoxy-matrix composite's resistivity in the fiber direction is essentially not affected by matrix damage and that in the through-thickness direction is not affected by slight matrix damage. In contrast, the carbon matrix is electrically conducting, so it allows matrix damage to be monitored electrically. Fatigue damage starts to be detectable electrically in the epoxy-matrix composite at about 50% of the fatigue life [11], but it is detectable in the carbon–carbon composite from the very first loading cycle onward, i.e., for the entire fatigue life.

The gage factor of the carbon–carbon composite is about equal to that of a single bare carbon fiber [37,40–44], which also increases in resistance upon tension due mainly to dimensional changes. However, a single carbon fiber [17] is not as effective a damage sensor as a carbon–carbon composite, since matrix cracking and fiber-matrix interface weakening cannot occur in a single carbon fiber. Furthermore, a single carbon fiber is not a structural material.

6. Conclusion

Self-monitoring structural materials constitute a class of structural materials that are intrinsically smart. The quantities monitored are strain and damage because of their relevance to structural control and structural health monitoring. These materials are self-monitoring because their electrical resistance or resistivity changes with strain or damage, such that strain causes a reversible resistance change and damage causes an irreversible resistance change. All self-monitoring structural materials are composite materials with fibrous reinforcements (continuous or discontinuous) that are at least as electrically conducting as the matrix. Three types of self-monitoring structural composites have been demonstrated. They are (i) composites with short fibers (e.g., cement mortar or concrete with short carbon fibers), (ii) composites with continuous fibers and non-conducting matrix (e.g., polymer-matrix composites with continuous carbon fibers), and (iii) composites with continuous fibers and conducting matrix (e.g., carbon-matrix composites with continuous carbon fibers).

Cement containing short carbon fibers (0.24 vol %) is a highly sensitive strain sensor, with a gage factor up to 700. The sensing ability stems from the reversible and slight fiber pull-out and the consequent reversible increase in the electrical resistivity.

A polymer-matrix composite containing continuous carbon fibers is a sensitive strain and damage sensor, with gage factor up to 38 in magnitude and with capability to detect fiber fracture and delamination. The strain sensitivity is due to the resistance in the fiber direction reversibly decreasing and that in the through-thickness direction reversibly increasing upon tensile loading in the fiber direction; the damage sensitivity is associated with the irreversible resistance increase in the fiber direction due to fiber fracture and in the through-thickness direction due to delamination.

A carbon–carbon composite with continuous carbon fibers is an exceptionally sensitive damage sensor, in addition to being a strain sensor. Even damage after the first cycle of tensile loading within the elastic regime was detected. The reversible resistance increase upon cyclic tension is mainly due to dimensional changes, but it is partly due to a phenomenon that intensifies as damage increases.

More self-monitoring structural materials and more origins of the self-monitoring ability are expected to be discovered in the next few years, as the field of self-monitoring structural materials is still in its infancy. Due to the infancy of this field, the various origins of the self-monitoring ability described in this review still need to be fully clarified by detailed scientific studies.

Acknowledgements

This work was supported in part by National Science Foundation.

References

[1] P.W. Chen, D.D.L. Chung, Smart Mater. Struct. 2 (1993) 22–30.
[2] P.W. Chen, D.D.L. Chung, J. Am. Ceram. Soc. 78 (3) (1995) 816–818.
[3] D.D.L. Chung, Smart Mater. Struct. 4 (1995) 59–61.
[4] X. Fu, D.D.L. Chung, Cem. Concr. Res. 25 (7) (1995) 1391–1396.
[5] P.W. Chen, D.D.L. Chung, Composites: Part B 27B (1996) 11–23.
[6] X. Fu, D.D.L. Chung, Cem. Concr. Res. 26 (1) (1996) 15–20.
[7] P.W. Chen, D.D.L. Chung, ACI Mater. J. 93 (4) (1996) 341–350.
[8] X. Fu, D.D.L. Chung, Cem. Concr. Res. 27 (9) (1997) 1313–1318.
[9] X. Fu, E. Ma, D.D.L. Chung, W.A. Anderson, Cem. Concr. Res. 27 (6) (1997) 845–852.
[10] X. Wang, D.D.L. Chung, Smart Mater. Struct. 5 (1996) 796–800.
[11] X. Wang, D.D.L. Chung, Smart Mater. Struct. 6 (1997) 504–508.
[12] X. Wang, D.D.L. Chung, Composites: Part B, 29 B (1) (1998) 63–74.
[13] S. Wang, D.D.L. Chung, Carbon 35 (5) (1997) 621–630.
[14] X. Wang, D.D.L. Chung, Smart Mater. Struct. 4 (1995) 363–367.
[15] X. Shui, D.D.L. Chung, Smart Mater. Struct. 5 (1996) 243–246.
[16] X. Shui, D.D.L. Chung, Smart Mater. Struct. 6 (1997) 1–4.
[17] N. Muto, H. Yanagida, M. Miyayama, T. Nakatsuji, M. Sugita, Y. Ohtsuka, J. Ceram. Soc. Jpn. 100 (4) (1992) 585–588.
[18] A. Ishida, M. Miyayama, H. Yanagida, J. Am. Ceram. Soc. 77 (4) (1994) 1057–1061.
[19] S. Wang, D.D.L. Chung, Smart Mater. Struct. 6 (1997) 199–203.
[20] P.W. Chen, D.D.L. Chung, Composites 24 (1993) 33–52.
[21] P. Chen, D.D.L. Chung, Composites: Part B 27B (1996) 269.
[22] L.A. Kuhlmann, Trans. Res. Record 1204 (1988) 52.
[23] X. Yang, D.D.L. Chung, Composites 23 (6) (1992) 453.
[24] N. Banthia, ACI SP-142, Fiber Reinforced Concrete, in: J.I. Daniel, S.P. Shah (Eds.), ACI, Detroit, MI, 1994, pp. 91–120.
[25] N. Banthia, A. Moncef, K. Chokri, J. Sheng, Can. J. Civ. Eng. 21 (1994) 999.
[26] V.C. Li, K.H. Obla, Composites Eng. 4 (9) (1994) 947.
[27] S.B. Park, B.I. Lee, Cem. Concr. Composites 15 (3) (1993) 153.
[28] P. Soroushian, M. Nagi, J. Hsu, ACI Mater. J. 89 (3) (1992) 267.
[29] H.A. Toutanji, T. El-Korchi, R.N. Katz, Cem. Concr. Composites 16 (1994) 15.
[30] K. Zayat, Z. Bayasi, ACI Mater. J. 93 (1996) 178.
[31] P. Chen, D.D.L. Chung, J. Electron. Mater. 24 (1) (1995) 47–51.
[32] P. Chen, X. Fu, D.D.L. Chung, ACI Mater. J. 94 (2) (1997) 147–155.

[33] P. Chen, X. Fu, D.D.L. Chung, ACI Mater. J. 93 (2) (1996) 129–133.
[34] X. Fu, W. Lu, D.D.L. Chung, Cem. Concr. Res. 26 (7) (1996) 1007–1012.
[35] X. Fu, W. Lu, D.D.L. Chung, Cem. Concr. Res. 26 (10) (1996) 1485–1488.
[36] X. Fu, W. Lu, D.D.L. Chung, Carbon, in press.
[37] X. Fu, D.D.L. Chung, Cem. Concr. Res. 25 (7) (1995) 1397–1402.
[38] X. Wang, D.D.L. Chung, Carbon 35 (5) (1997) 706–709.
[39] X. Wang, D.D.L. Chung, Carbon, 35 (10/11) (1977) 1649–1651.
[40] P.C. Conor, C.N. Owston, Nature 223 (1969) 1146–1147.
[41] A.S. Crasto, R.Y. Kim, Proc. Am. Soc. Composites, 8th Tech. Conf., Technomic Pub., Lancaster, PA, 1994, pp. 162–173.
[42] C.N. Owston, J. Phys. D. 3 (1970) 1615.
[43] C.A. Berg, H. Cumpston, A. Rinsky, Textile Res. J. 42 (8) (1972) 486.
[44] S.J. DeTeresa, Carbon 29 (3) (1991) 397.